TÜBİTAK

Turkish Journal of Physics

http://journals.tubitak.gov.tr/physics/

Invited Research Article

Turk J Phys
(2014) 38: 323 – 327
© TÜBİTAK
doi:10.3906/fiz-1405-5

Extended defects in GaN nanocolumns characterized by cathodoluminescence directly performed in a transmission electron microscope

Frank BERTRAM[1,*], Marcus MÜLLER[1], Gordon SCHMIDT[1], Peter VEIT[1], Jürgen CHRISTEN[1], Arne URBAN[2], Joerg MALINDRETOS[2], Angela RIZZI[2]

[1]Institute of Experimental Physics, Otto-von-Guericke-University Magdeburg, Magdeburg, Germany

[2]Fourth Institute of Physics, Georg-August-University Göttingen, Göttingen, Germany

Received: 09.05.2014 • **Accepted:** 19.06.2014 • **Published Online:** 10.11.2014 • **Printed:** 28.11.2014

Abstract: Using cathodoluminescence spectroscopy directly performed in a scanning transmission electron microscope at liquid helium temperature, the structural and optical properties of GaN nanocolumns, in particular extended defects like stacking faults and dislocations, have been characterized. The influence of the crystalline real structure on the emission properties using the capability of addressing individual stacking faults is comprehensively examined.

Key words: Scanning transmission electron microscope, cathodoluminescence, extended defects, basal plane stacking fault, GaN nanocolumns

1. Introduction

The controlled growth of GaN nanocolumns (NCs) offers a potential benefit for achieving higher efficiencies of III–V nitride-based optoelectronic devices due to a reduced density of structural defects, in particular dislocation, in comparison to planar heterostructures [1]. By taking advantage of the core-shell geometry of NCs with a high aspect ratio, the effective light-emitting area can be dramatically increased in comparison to conventional planar structures [2]. Furthermore, the growth of thin films on nonpolar and semipolar crystal planes of NCs minimizes the negative impact of polarization fields in comparison to c-planar structures.

For a clear understanding of the growth process of nanocolumnar heterostructures, as well as the incorporation of defects within NCs, highly spatially and spectrally resolved luminescence investigations of individual NCs are of high interest. This work reports on the direct nanoscale correlation of the optical properties with the actual real crystalline structure of single GaN NCs using low-temperature cathodoluminescence (CL) spectroscopy in a scanning transmission electron microscope (STEM).

The sample under investigation was grown by catalyst-free molecular beam epitaxy (MBE) on GaN(0001)/sapphire template. A 10-μm Mo mask was deposited by electron-beam evaporation on top of the template and regular arrays of circular apertures were patterned by electron beam lithography. Subsequently, the MBE process led to selective growth of GaN in the circular apertures providing regular arrays of hexagonal Ga-polar NCs with semipolar faceted tips [3]. The optimized cross-section transmission electron microscope (TEM) specimens for CL investigations were prepared by cutting a 2-μm-thick lamella from the NC array by focused ion beam (FIB). To protect the GaN NC during the FIB process, the NC array was embedded in a thick Si_3N_4 matrix and covered by a Pt stripe. Subsequently, an iterative FIB milling took place on the front and back side. Finally,

*Correspondence: frank.bertram@ovgu.de

an improved Ar+ ion milling process removing the amorphous surface caused by the FIB etching especially for CL led to a TEM lamella of 150–200 nm thick.

A comprehensive study of the structural and optical properties of GaN NCs has been realized by highly spatially resolved CL characterization. To achieve the highest spatial resolution in our study, we used liquid-He-temperature CL spectroscopy performed directly in a STEM ($\delta x < 1$ nm at RT, $\delta x < 5$ nm at 10 K) providing a unique, extremely powerful tool for correlated optical-structural nanocharacterization of single NCs, even in samples with high column density.

Our CL detection unit was integrated in a FEI (S)TEM Tecnai F20 equipped with a liquid helium stage (T = 10 K up to room temperature) and a retractable, light-collecting mirror. The emitted CL light was collected by this parabolically shaped mirror above the sample and focused onto the entrance slit of a grating monochromator. In STEM mode, the electron beam is convergent and either kept at a single position for local spectra or scanned over the region of interest in imaging mode. Panchromatic as well as spectrally resolved (grating monochromator) CL imaging can be performed using a highly sensitive photomultiplier. Alternatively, we were able to use a parallel detector for spectral imaging. The CL intensity was collected concomitant with the STEM signal at each pixel. The TEM acceleration voltage is optimized to minimize sample damage and prevent luminescence degradation under electron beam excitation (80 kV).

The cross-sectional STEM image in high-angle annular dark field contrast (HAADF) of the TEM lamella reveals a single NC (Figure 1a). One individual pencil-shaped GaN NC with semipolar facets at the very top has a diameter of about 200 nm and a height of 550 nm, respectively, leading to a given aspect ratio of 1:3. The GaN template, the Mo mask directly placed on top of the template, and the Si_3N_4 matrix enclosing the NC can be seen. Direct correlation of the HAADF image with the simultaneously recorded panchromatic CL mapping at 15 K (spectrally integral intensity in the wavelength range of 300–900 nm) exhibited the highest CL intensity exclusively from the GaN NC (Figure 1b, CL intensity image), in particular from the very center of the NC. In contrast, we did not observe CL intensity from the underlying GaN template, the Si_3N_4 matrix, or the Mo. The highest CL intensity came from the very center of the NC. It is noteworthy that the lamella surface areas of the GaN template were exposed to the milling process, whereas the NCs surfaces were protected by the Si_3N_4 matrix.

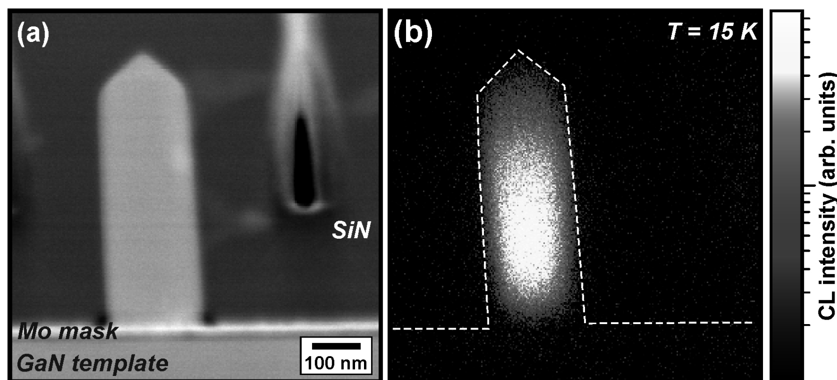

Figure 1. Low-temperature panchromatic STEM-CL mapping shows (a) HAADF contrast of GaN NC grown on a template and embedded in Si_3N_4 simultaneously recorded with a (b) panchromatic CL-intensity image (logarithmic scale). No extended defects are visible in the HAADF image. The GaN NC exhibits CL intensity exclusively. The low-temperature spectrum of this NC can be seen in Figure 2.

The spatially averaged CL spectrum (Figure 2) at a temperature of 15 K from the NC region displayed

in Figure 1 shows an intense (D^0,X) emission from GaN at $\lambda = 355.8$ nm, indicating a slightly compressive strain of the pillar. The spectral position of the (D^0,X) luminescence did not change along the NC length, suggesting the same strain state for the whole wire (not shown here). Furthermore, we observed weak, defect-related emissions between 365–405 nm, which clearly can be assigned to adjacent NCs that were not defect-free. Figure 3a contains a single NC with 3 individual stacking faults, which show a bright HAADF contrast extended parallel to the basal plane. Pinned at the surface, these basal plane stacking faults (BSFs) are not terminated by partial dislocations [4]. The first 2 BSFs have a shorter distance (Δx = 46 nm) between each other than the last one to the center BSF (Δx = 96 nm). The upper BSF terminated at semipolar facets in contrast to the 2 lower ones, which terminated at nonpolar facets. The highest CL emission in the intensity image is seen from the stacking faults (Figure 3b).

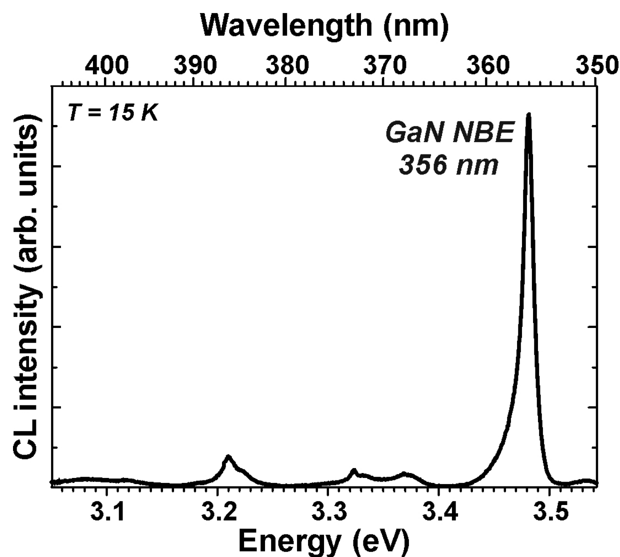

Figure 2. CL spectrum with linear scale of NC depicted in Figure 1 (T = 15 K). The luminescence is dominated by an intense near-band-edge emission of GaN (donor-bound exciton at $\lambda = 356$ nm).

Luminescence from the BSFs appears in the spectrum (Figure 3c). In contrast to the spectrum of Figure 2, a donor-bound exciton emission can be found at a spectral position of 356.2 nm. In addition, 2 luminescence peaks from the BSF type I_1 show up at $\lambda = 361.2$ nm and $\lambda = 362.3$ nm, respectively. Hence, the BSFs of the same type I_1 do not appear with a constant peak wavelength. A spectrally different BSF emission in one sample was already reported before in the experimental work of Bastek et al. [5]. A more detailed, highly spatially resolved analysis with local spectra exhibited a distinct peak wavelength for each of the 3 BSFs type I_1, starting at 361.2 nm for the lower BSF and 361.6 nm for the center BSF, and ending at 362.3 nm for the upper BSF (not shown here). We found a slight change of BSF emission energy of 10.5 meV over a distance of 140 nm.

Assuming the same constant strain conditions like for the NC in Figure 1, a strain gradient can be excluded to explain this wavelength change. One possible explanation for the characteristic emission might be the quantum mechanical coupling of all 3 narrow-laying BSFs, which can be seen as cubic quantum wells in a hexagonal matrix, and the effect of the quantum-confined Stark effect due to internal electric fields (spontaneous polarization). Nevertheless, the theoretical work by Corfdir et al. [6] comprehensively described the coupling between 2 adjacent BSFs and excluded an influence for distances of larger than 6 nm.

Furthermore, an inhomogeneous incorporation of impurities from the masking process, resulting in different free-carrier concentrations, can explain different emission energies of the BSFs.

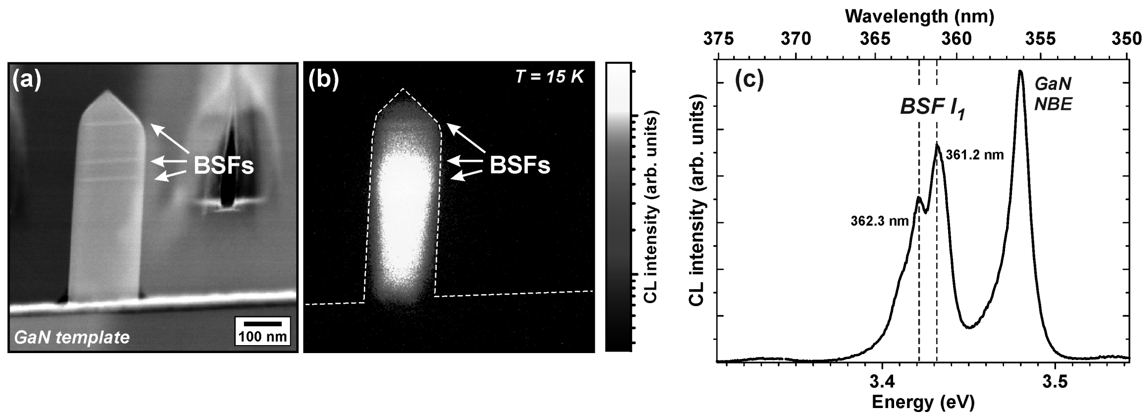

Figure 3. (a) HAADF-image, (b) panchromatic CL intensity image, and (c) optical spectrum taken at a low temperature of a GaN NC with 3 extended defects: the basal plane stacking faults of type I1 are marked in the HAADF image (a). The spectrum shows distinct luminescence of the donor-bound exciton as well as 2 peaks from the BSF I_1.

An even more complex situation can be seen in Figures 4a–4g (set of monochromatic images, Figures 4c–4g), where we have a single NC with a rich structure of stacking faults. The NC does not look pencil-like anymore. Instead, several different semipolar facets form the NC. BSFs with different distances can be found, as well as donor-bound exciton emission and luminescence from BSF type I_1 (361 nm) and type I_2 (373 nm), the extrinsic BSF E (377 nm), and thicker cubic inclusions (383 nm). The (D^0,X) emission is weak (Figure 4c) in comparison to that exhibited by the NCs in Figures 1 and 3. The BSF type I_1 luminescence can be obtained in Figure 4d and the BSF I_2 in Figure 4e, as well as BSF E in Figure 4f and cubic inclusions in Figure 4g.

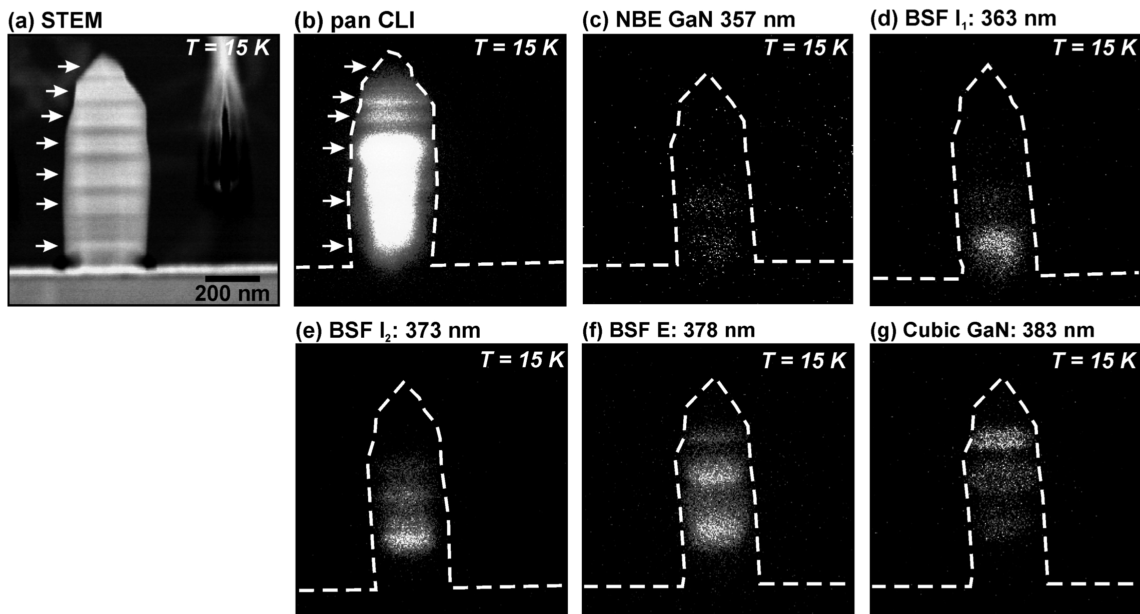

Figure 4. Series of monochromatic low-temperature STEM-CL mappings of a GaN NC with a rich defect structure. The positions of the extended defects are marked with white arrows in the ADF-STEM image (a). The spectrum of this column is depicted in Figure 5.

According to the rich defect structure, the spectrum of this NC exhibits a diverse spectral emission (Figure 5). (D^0,X), BSF I_1, BSF I_2, BSF E, and cubic GaN emission can be identified as isolated lines in the luminescence.

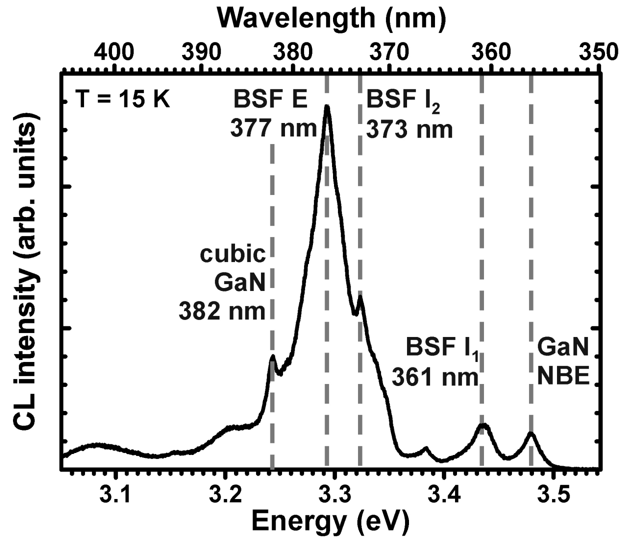

Figure 5. Low-temperature spectrum of NC depicted in Figure 4 (T = 15 K). The luminescence is dominated by the luminescence of extended defects.

In summary, we were able to address single to very few BSFs in individual GaN NCs. Each type of stacking fault is optically active and appears with a characteristic wavelength in the spectrum. Distinct emission lines were found, even for the same type of BSFs.

Acknowledgement

We gratefully acknowledge the German Research Foundation for its financial support in the frame of the Research Instrumentation Program INST 272/148-1 as well as the Collaborative Research Center SFB 787 "Semiconductor Nanophotonics: Materials, Models, Devices".

References

[1] Zubia, D.; Hersee, S. D. *J. Appl. Phys.* **1999**, *85*, 6492.

[2] Waag, A.; Wang, X.; Fündling, S.; Ledig, J.; Erenburg, M.; Neumann, R.; Al Suleiman, M.; Merzsch, S.; Wei, J.; Li, S. et al. *Phys. Status Solidi C* **2011**, *8*, 2296–2301.

[3] Urban, A.; Malindretos, J.; Klein-Wiele, J. H.; Simon, P.; Rizzi, A.*New J. Phys.* **2013**, *15,* 053045.

[4] Stampfl, C.; Van de Walle, C. G. *Phys. Rev. B* **1998**, *B57*, 15052.

[5] Bastek, B.; Bertram, F.; Christen, J.; Wernicke, T.; Weyers, M.; Kneissl, M. *Appl. Phys. Lett.* **2008**, *92*, 212111.

[6] Corfdir, P.; Lefebvre, P. *J. Appl. Phy.* **2012**, *112*, 053512.